Article:
Gottesmann, M, Goycoolea, FM, Steinbacher, T et al. (2020) Smart drug delivery against Helicobacter pylori: pectin-coated, mucoadhesive liposomes with antiadhesive activity and antibiotic cargo. Applied Microbiology and Biotechnology, 104 (13). pp. 5943-5957. ISSN: 0175-7598

https://doi.org/10.1007/s00253-020-10647-3

Research Paper

Smart drug-delivery against *Helicobacter pylori:* Pectin-coated, mucoadhesive liposomes with antiadhesive activity and antibiotic cargo

Maren Gottesmann[1], Francisco M. Goycoolea[2], Tim Steinbacher[3], Tamara Mengoni[4] and Andreas Hensel[1*]

[1] University of Münster, Institute of Pharmaceutical Biology and Phytochemistry, Corrensstrasse 48, 48149 Münster, Germany.

[2] University of Leeds, School of Food Science and Nutrition, LS2 9JT Leeds, United Kingdom

[3] Institute of Medical Biochemistry, University of Münster, Von-Esmach-Straße 56, Münster, Germany

[4] University of Münster, Institute of Plant Biology and Biotechnology, Schlossplatz 8, 48143 Münster, Germany

*** Correspondence:**

Andreas Hensel, Institute of Pharmaceutical Biology and Phytochemistry, University of Münster, Corrensstraße 48, 48149 Münster, Germany

Phone: +49 251 8333380, e-mail: ahensel@uni-muenster.de

Running Title: Smart liposomes against *H. pylori*

Date of acceptance: 26 April 2020

Published in *Applied Microbiology and Biotechnology,* 104, 5943–5957(2020)

https://doi.org/10.1007/s00253-020-10647-3

Abstract

The first step in the development of *Helicobacter pylori* pathogenicity is the receptor-mediated adhesion to the gastric epithelium. Inhibition of outer membrane proteins of *H. pylori* (e.g. BabA) by antiadhesive drugs will contribute to reduced recolonization and infection. Pectin from apple inhibits the BabA and LPS-mediated adhesion of *H. pylori* to human stomach cells. Pectin-coated liposomes with encapsulated amoxicillin were characterized for polydispersity, zeta potential, encapsulation efficiency, stability and amoxicillin release. Coated liposomes did not influence the viability of AGS and HT29-MTX cells up to 100 µg/mL but exert cytotoxicity against *H. pylori* at 10 µg/mL. Pectin-coating of liposomes provoked direct interaction and subsequent binding of the particles to surface structures of *H. pylori*, and interaction with mucus from porcine stomach and mucus secreted by HT29-MTX cells. Laser scanning microscopy of *H. pylori* and AGS cells together with liposomes indicated co-aggregation. The mucoadhesive effect seems interesting as stomach cells are covered by a mucus layer. *H. pylori* is able to penetrate and cross the mucin rapidly to reach pH-neutral epithelium to escape the acidic environment, followed by interaction with epithelia cells. Summarizing, all experimental evidence is consistent with a specific interaction of pectin-coated liposomes with mucins and surface structures of *H. pylori*. As the coated liposomes show mucoadhesion to the negatively charged mucins, docking to stomach mucin, mucus penetration, recognition of and adhesion to *H. pylori* they can be considered as a novel type of multi-functional drug carriers for local antibiotic therapy against *H. pylori*.

Keywords

Adhesion, bacterial antiadhesion, *Helicobacter pylori*, Liposomes, Mucoadhesion, Pectin

Key Points

- Smart, multifunctional liposomes
- mucoadhesive
- Specific targeting against BabA/LPS of *Helicobacter pylori*
- Inhibition of bacterial adhesion of H. pylori to human host cells
- Release of antibiotic cargo

Introduction

H. pylori infection rate is estimated worldwide with approximately 44 % of the human population, with highest prevalence in Africa and Latin America (Zamani et al., 2018). Standard therapy of the infection is clinically performed by a combination of different antibiotics, bismuth and proton-pump inhibitors, but high recurrence rates and increasing bacterial resistance against the standard antibiotics strongly limit the eradication (Malfertheimer et al, 2017). Development of resistant *H. pylori* can be related to improper use of the antibiotics, a short half-life time of the used antibacterial agents in the gastric compartment and also to the fact that the antiproliferative effects of these drugs is suboptimal against *H. pylori* which are mostly hidden in the mucus layer of the stomach, which is not easy to be penetrated by most antibiotics. It has to be pointed out that World Health Organization (WHO) lists clarithromycin-resistant *H. pylori* with a high priority for development of new antibiotics (WHO, 2017).

Most *H. pylori*-positive patients remain asymptomatic, but the infection is associated with an increased risk for peptic ulcer diseases, adenocarcinoma, and gastric lymphoma. Thus, in 1994, the WHO classified this bacterium as a group I carcinogen (International Agency for Research on Cancer IARC 1994). 65 to 80 % of gastric cancers are reported to test positive for *H. pylori* in non-cardia cancers (*Helicobacter* and Cancer Collaborative Group 2001; Sitarz et al. 2018), emphasising the pathogenicity of this bacterium.

Interestingly, recent reports have indicated that *H. pylori* in the gastrointestinal system can interact with orally administered drug medication. For example, levodopa, used for the treatment of Parkinsons's disease can be bound to outer membrane proteins of the bacterium, thus reducing the amount of the drug and therefore changing bioavailability and pharmacokinetics in *H. pylori*-positive patients (Niehues and Hensel 2009; Narożańska et al. 2014). Thus, novel treatment strategies or innovative drug delivery systems are required.

Outer membrane proteins (OMP), the so-called adhesins of *H. pylori*, are responsible for the specific recognition of the host cells and for the subsequent adhesion (for review see Ansari and Yamaoka, 2019). OMPs interact also specifically with the extracellular polymers of the mucin layer, anchoring the bacterium into the pH neutral area of the stomach. Adhesins can be targeted within new and innovative antiadhesive and cytoprotective strategies against the infection.

Initiation of the infection is mediated by bacterial recognition and adherence to the gastric epithelium, thus, antiadhesive compounds that inhibit this crucial docking process can be a promising and new approach.

Anti-adhesive compounds present a promising alternative for the prophylaxis and protection against *H. pylori* infections as they intervene in the first step of the development of its pathogenicity. However, the removal of already attached bacteria from the host cells is in general not possible solely under this approach. Thus, an antiadhesive strategy can only be considered for prophylaxis or for cytoprotection against recurrent *H. pylori* infections, but until now, no clear alternative to the current standard eradication regimen has been described. On the other hand, antiadhesive treatment could prevent new infections or recurrence, which is still a big problem in *H. pylori* clinical treatment, even after positive eradication therapy. For this, new strategies and targets should be considered, using innovative formulations, which increase the residence time of the antibacterial drug cargo in the stomach by interaction with the mucus layer, specifically interacting with bacterial virulence factors (Menchicchi et al. 2019). Previous studies have shown that both anionic polysaccharides such as dextran sulfate and cationic ones such as chitosan can interact with mucins (Menchicchi et al. 2015a) and some of these can also modulate adhesive interactions with *H. pylori* (Menchicchi et al. 2015b).

Historically, the identification of antiadhesive compounds against *H. pylori* is based on the initial findings on the antiadhesive properties of 3′-sialyllactose (Mysore et al. 1999). Unfortunately, this compound failed to prevent bacterial colonization of the human stomach in a clinical pilot study (Parente et al. 2003), because of a rapid degradation of the compound under physiological conditions in the stomach. The search for other antiadhesive compounds has yielded peptides (Niehues et al. 2010), *N*-phenylpropenoyl-L-amino acids (Hensel et al. 2007), polyphenols (Shmuely et al. 2004; Wittschier et al. 2007, 2009), and polysaccharides that interact specifically with carbohydrate-binding, lectin-like OMPs of *H. pylori* (Gottesmann et al. 2020); for review see (Menchicchi et al. 2015b). Interestingly, some antiadhesive, pectin-like polysaccharides additionally exert mucoadhesive properties (Gottesmann et al. 2020). This leads to the hypothesis that these polyfunctional compounds can in an initial first step stick to the mucus layer of the stomach, followed by mucus-penetration; subsequently the polysaccharide can get into physical contact with *H. pylori*, which in most cases are hidden in the pH-neutral mucin layer, followed by binding to the polysaccharide-sensitive OMPs (e.g. BabA, SabA, LPS). This again leads to the inhibition of the specific recognition and interaction with the eukaryotic host cell. This concept of combined mucoadhesive-antiadhesive compounds has recently led to the development of dextran sulfated nanocapsules, which inhibit the adhesion of *H. pylori* to human stomach cells under in vitro conditions. Follow-up studies in our group have pinpointed mucoadhesive and antiadhesive properties of a special apple pectin. To explore the potential of this rhamnogalacturonan, the present study aimed to evaluate the potential

performance of pectin-coated, antibiotic-loaded liposomes to interact with mucin, bind to *H. pylori*, release the antibiotic cargo and inhibit the bacterial adhesion to the host cells. From our point of view, such "smart" liposomes can provide an effective, cheap and innovative way for improved treatment of *H. pylori* infections. Therefore, the present study describes an effective technology for a multi-functional "smart" drug delivery system, which interacts specifically with the pathogen and releases a bactericidal drug in its direct surrounding so that the antibiotic dosage can be reduced. For this purpose, amoxicillin-loaded liposomes, coated with a negatively charged pectin have been developed.

Materials and Methods

Solvents, reagents, general experimentation procedures

If not stated otherwise, solvents, reagents, and consumables were obtained from VWR (Darmstadt, Germany, now Merck) or Merck KGaA (Darmstadt, Germany). Apple pectin (degree of esterification 38 %) was obtained from Carl Roth (Karlsruhe, Germany). Analytical characterization of the pectin was performed according to the methodology described elsewhere (Sehlbach et al. 2013; Herrmann et al. 2012). Sheep blood (defibrinated) was obtained from Oxoid (Wesel, Germany), fetal calf serum (FCS) was from Merck (Berlin, Germany).

Preparation of liposomes

Liposomes were prepared by thin-film hydration method, as described by (Weissman et al. 1965). Lecithin, cholesterol and didodeclydimethylammonium bromide (DDAB) (40:80:20) were dissolved in 6 mL chloroform/methanol (1:1, v/v). The organic solvent was evaporated by a rotavapor (150 mbar, 40 °C). The formed dry lipid film was resuspended in 10 mL phosphate buffered saline (PBS) and stirred in a water bath for 30 min at 40 °C. Finally, the liposomal suspension was sonicated for 30 min in an ultrasonic bath (Bandelin Sonorex RK102H, Bandelin, Berlin, Germany). The so formed uncoated liposomes (UCL) were dialysed (cellulose membranes, molecular weight cut off MWCO 300 kDa, Spectrum, Laguna Hills, USA) for 24 h against Aqua Millipore® (Merck, Darmstadt, Germany) and their size distribution and zeta-potential were characterised (see below). UCLs were stored at 2 to 8 °C for further use.

Coating of liposomes: UCL were coated with apple pectin solution (2 mg/mL) in a ratio of 1 of liposome suspension and 5 parts of the pectin solution (v/v). UCL suspension was added dropwise to the coating solution under continuous stirring (450 rpm). The resulting coated liposomal suspension (CL) was sonicated for further 15 min. To prove the successful coating, the size and zeta potential of CL were characterised (see below).

The absolute mass of the liposomes in suspension was determined by a gravimetric method. Briefly, 20 µL of the dispersion was transferred into a micro weighing vessel and dried at 80 °C for at least 4 h. For every liposomal suspension, a technical triplicate was performed.

Drug loading of liposomes: For drug loading of liposomes, the liposomes were prepared as described above, with a modified resuspension step. Instead of using only PBS for the hydration process, PBS containing 100 µM amoxicillin was used, thus resulting in the formation of uncoated-amoxicillin liposomes (UCL_A) and coated-amoxicillin liposomes (CL_A).

Fluorescence labelling of liposomes: UCL and CL were labelled with the fluorescence dye 1,1-dioctadecyl-3,3,3,3-tetramethylindodicarbocyanin (DiD, Thermo Scientific, Waltham, USA) (0.047 mM). Due to the lipophilic properties of DiD, the dye was incorporated into the hydrophobic phase of the liposomes after the addition of the dye to the organic solvent. The liposome preparation and the respective characterisation was performed as described above. In order to confirm the successful incorporation of DiD into the lipophilic part of the liposomes, free DiD was separated from the embedded dye by ultrafiltration (30 min, 12,000 × g) using Vivaspin® 500 centrifugal concentrators (MWCO 30 kDa, Sartorius, Göttingen, Germany). Unbound DiD that passed through the membrane of the Vivaspin® was determined by fluorescence spectroscopy.

Determination of size distribution and zeta potential

The size (hydrodynamic diameter) and the polydispersity index (PDI) were determined by dynamic light scattering with non-invasive back scattering (DLS-NIBS) at an angle of 173°, and the effect of the coating on the surface charge was determined by measuring the zeta potential by mixed-laser Doppler electrophoresis and phase analysis light scattering (M3-PALS). Both measurements were acquired using a Malvern Zetasizer Nano ZEN 3600 (Malvern Instruments, Malvern, UK) at 22 °C fitted with a laser output of 4 mW He/Ne operating at $\lambda = 633$ nm. Ten microliter of the test suspension were diluted with 990 µL Aqua Millipore®. The Zetasizer Software 7.13 was used to compute the Z-average hydrodynamic diameter and PDI by processing the correlograms and fitting the corresponding autocorrelation function.

Encapsulation efficiency (EE) of amoxicillin (by UPLC)

Non-encapsulated amoxicillin was separated from 500 µL of liposomal suspensions UCL_A and CL_A by Vivaspin® 500 (MWCO 30 kDa) centrifugal concentrators (2 × 30 min, 12,000 × g). Free amoxicillin that passed through the membrane of the Vivaspin® was quantified by UPLC. UPLC settings: Acquity™ Ultra Performance LC (Waters Milford, USA); stationary phase: HSS T3, 1.8 µm, 2.1 × 100 mm, 40 °C; mobile phase: binary gradient of (A) 0.1 % formic acid in water and (B) 0.1 % formic acid in acetonitrile, run time: 15 min, flow rate: 0.4 mL, $\lambda_{max} = 254$ nm.

The EE was calculated as:

Encapsulation efficiency $[\%] = \frac{Total_{amox}\text{-}Free_{amox}}{Total_{amox}} \times 100$

In vitro release study of amoxicillin

For characterization of the drug release from the liposomal delivery system, UCL_A and CL_A were incubated at 37 °C under shaking conditions (600 rpm) over 24 h in AGS cell culture medium. After different time intervals (15 min, 30 min, 1 h, 2 h, 4 h, 6 h and 24 h), samples were centrifuged at 20,000 × g for 16 - 18 h at 17 °C to separate liposomal components. The respective supernatant was used for quantification of released amoxicillin using UPLC (see above).

Stability of liposomes

UCL, CL, UCL_A and CL_A were stored in aliquots over three months at different temperatures (8 °C, room temperature (RT, 20 - 25 °C), and 37 °C). Every 4 weeks the size, the PDI and the zeta potential were determined.

Furthermore, the stability of UCL_A and CL_A in simulated gastric fluid (SGF, pH 1.2; 0.2 g NaCl, 0.32 purified pepsin (activity 800-2000 U/mg protein), 0.7 mL HCl, ad 10 mL water, adjust pH with hydrochloric acid) was tested over 24 h. Ten microliters of each suspension were mixed with 990 µL SGF and incubated for 1, 2, 3, 4, 6, and 24 h at 37 °C under shaking (300 rpm), followed by determination of particle size and PDI.

Cell culture

Human adherent gastric adenocarcinoma epithelial cells (AGS, ATCC CRL-1739™) were cultivated as described by Messing et al. (2014). HT29-MTX-E12 mucus-secreting epithelial cells (ECACC 12040401) were kindly donated by Prof. Dr. K. Langer (University of Münster, Germany) and cultivated at 5 % CO_2, 37 °C in HT29-MTX cell culture medium (Dulbecco's Modified Eagle's MediumDMEM 500 mL, FCS 10 % (v/v), Pen/Strep 1 %, gentamycin 1 % (v/v), non-essential amino acids 1 % (v/v). In case of HT29-MTX-E12 cells, experiments were carried out by either using 24 h cultured cells (exponential growth phase) or using 2 weeks old cells (confluent mucus-secreting monolayers).

Determination of cell viability

The cytotoxic influence of liposomes on AGS cells and HT-29 MTX cells was determined by a colorimetric assay for assessing cell metabolic activity by use of 3-(4,5-dimethylthiazol-2-yl)-2,5-diphenyltetrazolium bromid (MTT) (Mosmann 1983) with minor modifications to avoid decomposition of the liposomes, as the used surfactant DDAB, used for liposome preparation, interferes with eukaryotic cell membranes. The liposomal suspensions were diluted in Dulbecco's phosphate buffered saline (PBS) with Ca^{2+} and Mg^{2+} ($PBS^{+/+}$) instead of the non-supplemented medium$^{-/-}$, and the incubation time of the AGS cells with the test samples was reduced to 2 h.

Bacteria growth conditions, fluorescent-labelling

H. pylori J99 (ATCC 700824, identification for quality control by PCR for *vacA*, accession number AAD06400, and *cagA*, accession number AAD06073), were cultivated according to Messing et al. (2014) for two or three passages to minimise the risk of phase-variable switching of OMP genes. Bacteria were grown under microaerophilic conditions on tryptic soy agar supplemented with 5 % defibrinated sheep blood for 48 h at 37 °C. Labelling *of H. pylori* with fluorescein isothiocyanate (FITC) was performed as described by Messing et al. (2014).
Standard cultivation was routinely performed at 10 % CO_2, while test assays were performed at 5 %. CO_2. This reduced CO_2 concentration did not influence the viability of *H. pylori* J99, as the assay duration under these conditions was maximum 90 min. Additionally, these changed conditions will not have an influence on the outcome of the results, as all measured values were related to the untreated controls, which had been treated the same way as the test samples.

Determination of cytotoxicity against *H. pylori* (agar diffusion test)

Agar grown bacteria were harvested and suspended in PBS. This suspension was adjusted to an OD_{550} of 0.2 and spread on an agar plate. The inoculated plate was zoned into 4 to 5 areas. One BD Sensi-Disk® (BD Biosciences, Heidelberg, Germany) was placed in the middle of each zone. Twenty microliters of an amoxicillin solution (2.5 µg/mL) served as positive control. Incubation time was 72 h under microaerophilic conditions.

Mucin interaction study by microviscosimetry (Menchicchi et al. 2014)

Preparation of mucin solution: Pig gastric mucin type III (Merck KGaA, Darmstadt, Germany) was purified as described elsewhere (Menchicchi et al. 2014). Briefly, mucin powder was hydrated in ultrapure water (30 mg/mL) under vigorous stirring for 12 h at RT. Insoluble

particles were removed by centrifugation (30 min, 18,000 × g, 15 °C). The supernatant (soluble mucin) was used for all further experiments.

Preparation of polysaccharide-mucin mixtures: The relative viscosity (η_{rel}) of polysaccharide test solutions and a mucin solution was determined at 37 °C using an automated rolling ball microviscometer AMVn (Anton Paar, Ostfildern, Germany) with an inclination of 50 °. Solutions were diluted to a η_{rel} of ~ 2.0 (stock solutions). To achieve different composition ratios for the mass fraction of mucin relative to the total mass (f), the stock solutions of polysaccharide and mucin were mixed in respective proportions in the range from $f = 0$ (only polysaccharide) to $f = 1$ (only mucin). The resulting polysaccharide - mucin mixtures were allowed to equilibrate at 37 °C for 20 min by gentle shaking (400 rpm).

Viscosity of polysaccharide-mucin solutions: The dynamic viscosity of the different composed mixtures was determined as described above. To assess the potential interaction between the polymers, a theoretical additive line (line of no interaction) (Hassan and Gallo 1990; Goycoolea et al. 1995) was calculated according to (Menchicchi et al. 2014). The difference between the theoretical viscosity and the viscosity determined experimentally ($\eta_{exp(f)}$) was expressed as a percentage deviation from the line of no interaction (Menchicchi et al. 2014):

$$\text{Deviation } [\%] = \frac{\eta_{t(f)} - \eta_{exp(f)}}{\eta_{t(f)}} \times 100.$$

Interaction of liposomes with HT-29 MTX cells

To investigate the interaction between liposomes and mucus in an in vitro model, the mucus-secreting cell line HT29-MTX was used. The development of this assay was inspired by (Adamczak et al. 2016). HT29-MTX cells were cultivated for 7 days in a black 96-well plate with a transparent bottom. The cell culture medium was changed every day. Seven days after the formation of a substantial mucus layer, the cells were washed with 200 µL PBS/well and with 200 µL Hanks' Balanced Salt Solution (HBSS) per well. Subsequently, 100 µL DiD-labelled liposomes (coated and uncoated, concentration 0.01 to 1 mg/mL) were added per well and incubated for 2 h at 37 °C, 60 rpm, under direct light exclusion. After 2 h, the test dispersions were removed and each well was washed with 200 µL HBSS to remove non-interacting liposomes to exclude false positive interaction between the mucus layer and the liposomes. The interaction was determined by fluorescence (λ_{ex} = 646 nm, λ_{em} = 678 nm). Cell-free wells, incubated with fluorescence-labelled liposomes, served as negative control to

monitor the adhesion of the liposomes to the abiotic surface. The relative mucus-interaction was calculated as follows:

$$\text{Relative mucus-interaction [\%]} = \left[\frac{F_1}{F_0} \times 100\right] - \left[\frac{F_A}{F_{0A}} \times 100\right]$$

F_1 fluorescence of liposomes interacting with mucus (after incubation and after washing)

F_0 fluorescence of liposomes in wells with cells before incubation

F_A fluorescence of liposomes in wells without cells after incubation and after washing

F_{0A} fluorescence of liposomes in wells without cells before incubation

Fluorescence microscopy

FITC labelled *H. pylori* J99 ($OD_{550} = 0.1$ in PBS) were added to DiD-labelled UCL and CL in a ratio of 1:4000. Five microliter of FITC-labelled bacteria, 5 µL of DiD-labelled liposomes, and 5 µL of the bacteria-liposome composition were mixed with 5 µL of Fluoromount™ mounting medium (Sigma Aldrich, St. Louis, USA). The suspension was transferred onto microscopy glass slides, which had been thoroughly cleaned with EtOH, and then sealed with a coverslip and nail polish. Microscopy samples were analysed by a Keyence BZ-9000 fluorescence microscope (Kyence, Neuisenburg, Germany). Unlabelled bacteria and unlabelled liposomes were prepared in the same manner to exclude auto-fluorescence of the samples.

Confocal laser scanning microscopy (CLSM)

Microscopy glass slides with a special microscopy 8-well chamber were coated (1 h, RT) with 200 µL/well collagen type 1 (BD, Heidelberg, Germany) solution. Each well was washed twice with 200 µL PBS. Depending on the experimental design either (A) 200 µL of an AGS cell suspension (5×10^5 cells/mL) or (B) 200 µL of a FITC-labelled *H. pylori* suspension ($OD_{550} = 0.3$ in blocking buffer) was added to each well.

A. The microscopy chambers containing AGS cells were incubated for 48 h at 37 °C. Cells were washed once with $PBS^{+/+}$ and non-supplemented $medium^{-/-}$ was added. 200 µL/well of FITC-labelled *H. pylori* suspension (optical density $OD_{550} = 0.1$ in PBS) were added and incubated with AGS cells (1 h, 37 °C). Non-attached bacteria were removed by 2 × washing with 200 µL/well $medium^{-/-}$. Coated and uncoated DiD-labelled liposomes were added in a ratio of 4000 : 1 (liposomes : bacteria). Therefore, the liposomal suspensions were diluted with $medium^{-/-}$. After 2 h incubation at 37 °C, unbounded liposomes were removed by washing twice with 200 µL/well $PBS^{+/+}$.

B. Two hundred microliter of a *H. pylori* suspension (OD_{550} = 0.1 in PBS) were incubated on collagen coated microscopy glass slides for 1 h at 37 °C. Prior to the addition of DiD-labelled liposomes (4000 : 1), each well was washed with 200 µL medium$^{-/-}$ to remove unbounded bacteria. The liposomes were incubated with the bacteria for 2 h at 37 °C and subsequently washed with 200 µL PBS$^{+/+}$.

For fixation of the samples, 200 µL of a paraformaldehyde solution (4 %) were added (15 min, RT). After 2 washing steps with 200 µL PBS$^{+/+}$, cells were stained for 30 min at RT in the dark with DAPI (1 µg/mL). Before the samples were covered with cover glasses, each well was washed again twice with 200 µL PBS$^{+/+}$ to remove unbounded dye. The microscopy chamber was removed carefully and the glass slide was washed once with Aqua Millipore® (Merck, Darmstadt, Germany). Once the slide was dry, Mowiol 4-88 served as mounting medium and was placed dropwise on every sample well, before the cover slide was put on. The preparations were kept overnight in the dark at 2 - 8 °C.

Microscope: LSM 800 with airyscan (Carl Zeiss, Jena, Germany) equipped with the objective Plan-Apochromat x63/1.4 oil; Microscopy slide: µ-slide 8well (Ibidi, Martinsried, Germany). Excitation and emission wavelengths λ [nm]: DAPI 405, 420-480; DiD 633, 665; FITC 488, 500-580.

Statistical analysis

Results are expressed as mean value (MV) ± standard deviation (SD). Mean values were compared by a one-way ANOVA test followed by a Tukey's test for multiple comparisons. A p-value < 0.05 compared to the negative control was considered statistically significant. IC_{50} values were calculated with GraphPad Prism® Vers. 7 (GraphPad Software, Inc., La Jolla, USA).

Results

Preparation and characterisation of liposomes

Liposomes were prepared by hydration of a lipid film and subsequent extrusion (Weissman et al. 1965). For this, a lipid film, composed of soy lecithin, cholesterol (for improvement of stability and reduced permeability of water-soluble molecules through the liposomal membrane) and DDAB was prepared by controlled evaporation of the chloroform/methanol solvent. Upon the addition of the aqueous dispersion medium (PBS), a liposomal suspension

was formed, from which after sonication homogenous, cationic DDAB liposomes were obtained (Supplementary Data Fig. S1). In the following sections, this preparation was named as UCL.

To obtain mucoadhesive liposomes with a conferred specific affinity against BabA of *H. pylori*, UCL were coated with apple pectin. The pectin was characterised by a galacturonic acid content of 84 %, degree of acetylation of 0.4 % and a degree of methyl ester content of 12.4 % using standard methods of polysacharide chemistry (Sehlbach et al. 2013; Herrmann et al. 2012). The full characterisation data (neutral and acidic carbohydrates, molecular weight, protein content, linkage analysis) are summarized in Supplementary Table S1. Using this polysaccharide for UCL coating, so-called CL were prepared. Additionally, amoxicillin was encapsulated either in UCL or in CL (named in the following as UCL_A or CL_A). Table 1 summarises the physicochemical properties of the so obtained liposomal formulations.

Both CL and CL_A had an appreciable higher hydrodynamic diameter (≥ ~500 nm) compared to UCL and UCL_A (≥ ~150 nm), thus reflecting the presence of the polymeric coating. Furthermore, inversion of charge was observed from positively charged UCL to negatively charged CL after covering the particles with the anionic rhamnogalacturonan. The PDI of UCL and CL was ≤ ~ 0.3, indicating a homogenous particle distribution (Dragicevic-Curic et al. 2008; Danaei et al. 2018).

Similar tendencies were obtained for DiD-labelled UCL and CL formulations used for further fluorescence microscopic investigations (Table 1). The so obtained particles were named in the following as UCL_DiD and CL_DiD. As expected, the size of the liposomes increased from ~140 nm to about ~430 nm after coating, while the respective PDI remained ≤ ~0.3 in both cases. Additionally, the surface charge changed from positive (+ 43.4 ± 5.0 mV for UCL_DiD) to negative (- 24.1 ± 0.9 mV for CL_DiD) values.

After labelling with DiD, the liposomes were, as expected, blue coloured. In order to confirm the successful association of DiD into the lipophilic part of the liposomes, free DiD was removed by ultrafiltration. Subsequently, the fluorescence within the remaining liposome pellet and the filtrate solution was quantified (data not shown), indicating that DiD has been incorporated completely into the liposomal formulations.

Stability of liposomes

In order to evaluate the short-time stability of liposomes during storage, the particles were stored over 3 months at different temperatures (8, 25 and 37 °C). As displayed in the Supplementary Fig. S2 and S3, uncoated liposomal formulations did not show any relevant

changes over the test period. The hydrodynamic diameter of UCL remained constant over the storage time (range 125 to 135 nm). The size of the corresponding amoxicillin-loaded liposomes was in the range of 140 to 160 nm. PDI for both, uncoated and coated formulations was ≤ 0.2 and the zeta potential remained stable over the storage time (range about + 50 ± 5 mV).

For pectin-coated liposomes the respective particle size was slightly affected by the three months storage period, while no noticeable changes of PDI (≤ 0.3) and zeta potential (- 32 ± 5 mV) were observed. After one month of storage at 8 °C, the size of CL increased from 400 to 430 nm (+ 7.5 %), while the size of CL_A increased from 410 to 470 nm (+ 14.6 %). After further storage at 8 °C, the liposome sizes decreased (CL after 3 months storage: 380 nm; CL_A: 440 nm). Storage at RT or 37 °C resulted in a constant, but moderate decrease of size over the 3 months period, which might be due to the coating solution being partially sheared off.

Furthermore, changes in the size of UCL_A and CL_A liposomes during incubation in SGF were determined by an in vitro assay to infer about the potential stability of the liposomal formulations in the gastrointestinal tract. As displayed in Fig. 1 the size and the respective PDI of UCL_A were not affected by the simulated gastric conditions over 24 h of incubation. However, the size of CL_A decreased within 60 min from 520 to 480 nm. Within 24 h the particle size of the coated formulation was reduced to 300 nm, while the PDI simultaneously increased, indicating liposomal decomposition.

Encapsulation efficiency (EE) and in vitro release of amoxicillin

For determination of the concentration of amoxicillin incorporated into the formulation, non-encapsulated, free amoxicillin was separated from the liposomes by ultrafiltration and was quantified by UPLC at λ = 254 nm against external calibration. EE was calculated from the difference in the total amount of amoxicillin used for manufacture of the liposomes and the amount of non-encapsulated, free amoxicillin, removed from the liposomes by ultrafiltration. The determined amoxicillin EE values for UCL_A and CL_A were 66 and 83 %, respectively. Subsequently, the in vitro release of the drug from the liposomes was determined by referring the data to their respective EE. Uncoated (UCL_A) and polymer coated (CL_A) amoxicillin delivery systems are characterized by an initial burst release profile (Supplementary Data Fig. S4). After 1 h, UCL_A released 85 % of the total drug cargo, followed by a plateau. 85 % release of UCL_A referred to 66 % EE corresponds to 56.1 µM amoxicillin. Coated formulations released about 75 % of the encapsulated amoxicillin after 60 min. Within this

time, CL_A also reached a plateau of release. The maximal release of CL_A corresponds to 62.3 µM amoxicillin.

Concluding, CL_A released ~10 % more amoxicillin compared to UCL_A, even though the curves in Supplementary Data Fig. S4 may seem to indicate a higher amoxicillin release of UCL_A. In fact, the observed differences lied within the experimental error of the determination.

Influence of liposomes on viability of HT29-MTX and AGS cells

The different liposomal formulations were investigated for their influence on the viability (Mosmann 1983) of human gastric AGS cells and human intestinal, mucin-secreting HT29-MTX cells (Lesuffleur et al. 1993).

Independent of the amoxicillin´s EE, uncoated and coated liposomes showed similar results on the viability of AGS cells (Fig. 2). A concentration of 0.5 mg/mL UCL and UCL_A significantly reduced the cellular viability to ~ 60 %, while liposomes at lower concentrations (0.01 and 0.1 mg/mL) had no influence on viability. A similar result was also obtained for CL and CL_A. It was observed that coating of the particles with the polysaccharide resulted in a slightly reduced decrease of cell viability compared to the uncoated formulations (≥ 70 % cell viability for 0.5 mg/mL CL and CL_A). Thus, for all further experiments liposomes concentrations < 0.5 mg/mL were used.

Fig. 3 displays the influence of the different nanocarriers on the cell viability of HT29-MTX cells. Different stages of growth of HT29-MTX cells were studied. Considering the initial exponential growth phase of the cells (Fig 3A), none of the liposomal formulations at ≤ 0.1 mg/mL did exert cytotoxic effects. Concentrations ≥ 0.5 mg/mL reduced the viability significantly. Testing amoxicillin loaded and unloaded UCL and CL in a concentration range of 0.01 to 1 mg/mL on mucus-secreting HT29-MTX cells (Fig 3B) did also not provoke significant cytotoxic effects, except for UCL and CL_A at a concentration of 1 mg/mL.

Direct cytotoxicity of liposomes against *H. pylori*

In order to evaluate the different lipidic nanocarrier systems in regards to their potential cytotoxic effects against *H. pylori*, disk diffusion assay was performed. UCL_A and CL_A were tested in a concentration range of 1 mg/mL to 0.01 mg/mL. For both formulations, a concentration-dependent effect on bacterial growth was observed. The zone of inhibition determined was comparable for both, coated as well as for uncoated formulations (Supplementary Data Table S2).

No cytotoxic effects were observed for the antibiotic-free liposomes UCL and CL. As expected amoxicillin-loaded liposomes provoked a concentration-dependent inhibition of *H. pylori*.

Interaction between liposomes and mucin

Stomach epithelial cells are covered by a mucus layer. *H. pylori* is able to penetrate and cross this viscous mucus layer of the gastric mucosa rapidly to reach the pH-neutral epithelium surface below the mucus layer, so that the pathogen can escape the acidic environment of the stomach and can interact with the stomach epithelia cells (Algood and Cover 2006).

To investigate if the liposomes are able to interact with the mucus, and thus reach the dormant *H. pylori* located in the mucus layer or on the host cell surface, the potential interaction between the nanoparticles and mucus was examined. To this end, both soluble mucin from porcine stomach and mucus secreted by HT29-MTX cells, were incubated during two hours with the liposomal formulations and the changes in size and zeta potential were evaluated.

Fig 4 displays changes in size and zeta potential resulting from the interaction between porcine mucin and amoxicillin-loaded liposomes. The corresponding values are displayed in the Supplementary Table S3. Within protocol 1 the liposomal suspensions were mixed at room temperature with a mucin solution (0.4 mg/mL) in a ratio of 1:1 (v/v) (Fig. 4A, B), followed by determination of the size and the zeta potential. In the second protocol 2, UCL_A and CL_A were incubated with 0.2 mg/mL mucin solution (ratio 1:1) for 2 h at 37 °C under gentle shaking (Fig 4C, D) to mimic the physiological conditions prior to the determination of physicochemical properties by DLS.

Both protocols indicated similar tendencies. Using protocol 1, the size of UCL_A increased from 151 to 624 nm. Within protocol 2, the size increased from 160 to 404 nm. For CL_A the initial size was already ~500 nm. After mixing CL_A with artificial mucin solutions, the size increased in both protocols to ~ 710 nm, which means an increase by a factor of 1.4. Interestingly, the PDI from UCL_A doubled after incubation with mucin in both protocols, while the PDI for CL_A remained stable.

Besides the size and PDI, the changes in the zeta potential were pronounced. Mucin is negatively charged at neutral pH and the saccharide chains of mucin polymers are characterised by a high amount of sialic acid (pK_a ~ 2.6) and sulfate (pK_a ~ 1) (Waigh et al. 2002), while glutamic and aspartic acid residues are present in the protein backbone (pK_a ~ 4) (Cao et al. 1999). The zeta potential of the mucin was determined with - 15 mV. Irrespective of the protocol performed, the surface charge of UCL_A was strongly reduced after contact with the different mucin preparations from $\geq +$ 40 mV to $\leq +10$ mV. For CL_A the zeta potential

changed by ~50 %. After incubation with mucin, the negatively charged CL_A showed a zeta potential of -16 mV, which is similar to that of the pure mucin solution used. Essentially similar results were obtained regardless of the used protocol.

In summary, contact of UCL_A or CL_A with porcine mucin resulted in a notable increase of size and a pronounced change of the zeta potential, both results providing unequivocal evidence of an interaction between both partners.

Subsequently, an in vitro model with HT29-MTX cells was used to study potential mucus-interacting properties of the liposomal formulations. This model allows the measurement of interactions between human cellular mucus, secreted from HT29-MTX cells and fluorescently labelled UCL and CL. (UCL_DiD and CL_DiD). Fig. 5 represents the interaction between HT29-MTX cells and different concentrations of DiD-labelled UCL and CL. As expected, the positively charged UCL_DiD interacted in a concentration-dependent manner with the HT29-MTX mucus. In addition, the negatively charged CL_DiD showed clear interaction with the mucins in a concentration-dependent manner, although not as intensively as determined for UCL_DiD. Comparing both formulations, CL_DiD interacted ~50 % less with the mucus than UCL_DiD at all concentrations used.

Interaction study between liposomes and *H. pylori*

To achieve a specific targeting of *H. pylori* by the liposomes, an interaction between the drug delivery system and the pathogen is a prerequisite. Fluorescence microscopic investigations were performed to determine if a specific targeting can be obtained by the liposome particles. The necessity of the coating with pectin was of particular interest, as it is known that the rhamnogalacturonan strongly and specifically interacts with the bacterial surface via BabA and LPS (Gottesmann et al. 2020).

In order to obtain an estimate on a possible interaction between the pectin-coated liposomes and *H. pylori* fluorescence microscopy imaging was performed, using DiD-labelled UCL and -CL together d with FITC-labelled *H. pylori*. Fig. 6 displays representative fluorescence images of bacteria in combination with the liposomes. FITC-labelled bacteria get obvious as green-coloured spots, while DiD-labelled liposomes are coloured in red. Co-localisation of liposomes together with bacteria should result in typical yellow colour. As expected, the combination of UCL_DiD together with bacteria revealed no specific interaction between pathogen and liposomal formulations, as only individual red and green spots were detected. In contrast, mixtures of CL_DiD and *H. pylori* revealed yellow spots, evidencing co-localisation and thus supports the assumption of a direct interaction between pectin-coated liposomes and bacteria.

More detailed investigations on the interaction between the liposomes and *H. pylori* were performed using confocal laser scanning microscopy (CLSM) using two different protocols. Under the first one, AGS cells were directly grown on microscopy slides and incubated with FITC-labelled *H. pylori,* followed by incubation with DiD-labelled UCL and CL. Fig 7 displays representative orthogonal projection CLSM images obtained during this experiment. In case of UCL no co-localisation between bacteria and liposomes was observed, as the fluorescence signals of liposomes and *H. pylori* are clearly separated. In contrast, bacteria, which had been incubated with CL, showed a mixed yellow colour, thus indicating an interaction between pectin-coated liposomes and *H. pylori,* attached to the AGS cells. These findings are in alignment with the previous insights obtained by the conventional wide-field microscopy.

Optical sectioning was used to generate a three dimensional image of the specimen, which clearly confirmed the above described results, as co-localisation of liposomes and bacteria was only observed in case of CL formulations; uncoated liposomes did not at all interact with *H. pylori* (Fig. 8).

Under the second protocol (Fig 9) no interaction of UCL with the bacteria were detected: After a 2 h incubation of *H. pylori* together with UCL and removal of unattached liposomes, no red colour was visible, indicating the absence of any interaction. In contrast, under identical assay conditions, the red-dyed CL could be clearly detected and presented the same shape as the blue-dyed bacteria. Consequently, a direct interaction between CL and *H. pylori* was obvious.

Discussion

Liposomes are sphere-shaped aqueous-core vesicles consisting of one or more lipid bilayers, with phospholipids (e.g. lecithin in our study) as building blocks. In order to modulate lipid composition and charge cholesterol and the quaternary ammonium DDAB had been embedded into the lipid bilayer. The addition of cholesterol reduces the permeability of the lipid bilayer and increases fluidity and stability of the membrane (Guyer and Bloch 1983). The addition of DDAB results in a positively charged particle surface, interacting more effectively with the negatively charged pectin. The successful coating was demonstrated by an increase in size and inversion of charge compared with UCL.

Charged liposomes, positively or negatively, have several advantages compared to neutral liposomes. The lack of surface charge (neutral liposomes) increases the aggregation and

flocculation of liposomes, as their physical stability is reduced. Thus, surface characteristics have a great impact on the stability of liposomes. In the literature, positive or negative zeta potential ≥ 30 mV have been reported to be sufficient for electrostatically stabilised suspensions (Cho et al. 2000). Within the present study, the stability of liposomes was monitored by controlling the physicochemical properties, such as size, PDI, and zeta potential. The liposomal formulations prepared within this study had cationic (uncoated) or anionic (coated) surface characteristics. Ideally, liposomes are designed to be stable during systemic circulation until they reach the target site (e.g., in cancer therapy). Upon interaction with the appropriate compartment in the target cells, the cargo should be rapidly released. In the case of liposomal formulations targeted to *H. pylori*, the stomach is the site of action. Therefore, an oral administration of the liposomes is to be preferred, as the formulation directly reaches the gastric environment. The stability of the liposomal formulations in the stomach was confirmed by assessing their size during incubation in simulated SGF. Interestingly, the uncoated system was stable under these acidic conditions over a 24 h period, while the coated liposomes showed a significant decrease in size and an increase in PDI after 2 h. We assume that under the acidic conditions and in the presence of pepsin, the pectin coating is sheared off from the lipid bilayer. The instability of liposomal vesicles in the gastrointestinal tract often limits the application of liposomal drug delivery systems as oral delivery carriers. It is known that gastric acid, bile salts and lipases reduce concentrations of intact liposomes and can therefore lead to uncontrolled cargo leakage (Rowland and Woodley 1980). On the other side bile and lipases are only relevant in the intestinal phase, not in the gastric area, where *H. pylori* is located. As the lipid bilayer itself was stable under the simulated gastric conditions, changes in lipid composition would probably not improve the stability of the pectin-coated liposomes in SGF, thus other strategies have to be considered.

Nevertheless, the site of action for the liposomes targeting against *H. pylori* is the acidic stomach, thus, a release of active compound in this compartment is desirable. Active ingredients, either encapsulated in the aqueous core of the liposomes (hydrophilic cargo) or integrated into the bilayer (lipophilic active ingredient), can be released from the liposomal formulations via erosion of the membrane, osmotic pumping or diffusion (Fredenberg et al. 2011). Therefore, a degradation within this environment is acceptable as it supports the release of the active agent. Within this study, the release of encapsulated amoxicillin from uncoated and coated liposomal formulates was compared. The results revealed that in total, coated liposomes released ~10 % more amoxicillin during a 24 h period compared to UCL. This apparently higher released amount of active drug, however, showed no differences regarding

the bactericidal activity of liposomes against *H. pylori*. Even though the anti-*H. pylori* activity was comparable, one reason for the increased release of amoxicillin from CL might be the destabilisation of the coated liposomes under acidic conditions; however, it has to be considered that the total EE of amoxicillin was higher and less variable in the polymer-coated system than in the uncoated one. It seems that the polymer coating has a positive effect on the capability of the liposome to encapsulate amoxicillin. It can be assumed that the polymer coating hinders a potential drug leakage from the inner core by forming an additional layer on the lipid membrane. Another reason for the greater encapsulation efficiency might be caused by the additional entrapment of the hydrophilic active drug into the polar pectin layer, which would lead to a two-staged release, initially a release of the active ingredient from the coating layer, followed by the release of the drug material, incorporated in the inner core. This additional embedding mechanism can be disregarded, as the in vitro release data of coated liposomes exhibit the same profile as that observed from the uncoated liposomes.

Another aspect that needs to be considered during the development of liposomes is their biocompatibility. In the case of the liposomes, this was assessed using viability test with different cell lines. UCL as well as CL at concentrations ≥ 0.5 mg/mL significantly reduced the viability of AGS and HT29-MTX cells. This might be due to degradation of the liposomal systems, leading to a release of the cell toxic quaternary ammonium salt DDAB. Nevertheless, it has to be considered that the gastric epithelial cells are covered by a thick mucus layer, hence direct contact between liposomes and cells is unlikely to occur. Furthermore, the mucus layer forms a physical barrier and has cell-protective qualities (Cornick et al. 2015). This characteristic was confirmed within this study, as no cytotoxic effect on HT29-MTX cells was observed when their self-secreted mucus layer covered them after 7 d of cultivation.

For a specific targeting of *H. pylori*, the interaction between the bacterium and the drug delivery system is important. For this, electrostatic interactions may also play an important role. (Nogueira et al. 2013) studied the effects of the gastric environment on *H. pylori* and showed that in acidic conditions the bacterium exhibits a positively charged surface (+ 20.0 mV at pH 2.6), while with increasing pH the surface became less positively charged (+ 0.7 mV at pH 4; - 6.6 mV at pH 6). The stomach presents an acidic environment even though *H. pylori* is colonised, thus negatively charged nanocarrier systems would be preferred for creating electrostatic interactions with the bacterial cells. However, *H. pylori* normally increases the pH in its direct surrounding by means of its urease until it reaches the more or less neutral mucosa close to the gastric epithelial cells, where it resides. Thus, the bacterium is generally exposed to neutral zones, which comes along with a slightly negative surface potential. Based on these

findings, positively charged drug delivery systems seem to present a better option for an electrostatic *H. pylori* targeting, as is has been demonstrated in previous studies between chitosan-coated nanocapsules and *Escherichia coli* (Qin et al. 2017). Nevertheless, within the present study, the pectin-coated, anionic liposomes have shown a clear co-localisation with the bacteria as determined by fluorescence microscopy. This had not been observed in case of the uncoated liposomes. Electrostatic interactions alone are not sufficient for a specific interaction between bacteria and nanocarrier. We assume that the interaction of the rhamnogalacturonan from the liposome-coating with the bacterium is not mainly due to electrostatic or ionic interactions, but much more related to a specific carbohydrate-protein interaction with the carbohydrate-binding "crown" of BabA, which normally interacts with the neutral carbohydrates of the blood group antigene Lewis(b) (Hage et al 2015). Bardonnet et al. (2008) proposed that besides electrostatic interactions, the presence of cholesterol is essential for an interaction between liposomes and *H. pylori*, as a specific affinity of the bacterium to this steroid has been described previously (Trampenau and Müller 2003). This cannot be the decisive factor for a specific interaction as in the present study both systems contain cholesterol, while only the coated one shows a significant interaction with *H. pylori*. Thus, a direct interaction with the bacterial surface, as it was shown for pectin, seems to be critical. So far, published studies have used fucosyled glycolipids (Bardonnet et al. 2008), fucose-conjugated chitosan (Lin et al. 2013) or the lectin concanavalin A (Ramteke et al. 2008) in order to achieve a specific interaction with *H. pylori* by interacting with the BabA adhesin (fucose) or by binding to carbohydrates on the surface of *H. pylori* (lectin). A recent study also investigated AGS cell membranes (Angsantikul et al. 2018) as coating system for nanosystems to achieve a specific targeting of *H. pylori*. This coated nanoformulation might be highly specific for *H. pylori* infections, however, the production is laborious and possible side effects have to be considered. The cost efficient and biocompatible apple pectin, used in the present study, represents a potential alternative for specific targeting of *H. pylori*. It is available in large scale and does not only interact with the BabA adhesin, but also interferes with the LPS of the bacterium. Furthermore, it exerts mucoadhesive properties, which supports the targeting of bacteria in the gastric mucosa.

From these experiments, evidence is consistent with a specific interaction of pectin-coated liposomes with surface structures of *H. pylori*. As the coating of the liposomes with pectin additionally provokes mucoadhesion to the negatively charged mucins, docking of the nanoparticles to stomach mucin followed by mucus penetration, recognition of and adhesion to *H. pylori* as well as release of the amoxicillin cargo, Summarizing, the mucoadhesive liposomal

formulation developed here presents an effective and novel type of multi-functional drug carrier system promising carrier system to deliver antimicrobial drugs specifically to *H. pylori*. It has several advantages over other nanoformulations that have been published so far. However, further studies with the apple pectin coated liposomes are yet to be conducted, especially the modification of the coated liposomes with an additional chitosan layer. The anti-adhesive formulations could also be used to facilitate eradication quadruple therapy, by making it more difficult for the bacteria (in the presence of antibiotics) to hide underneath the mucus layer where antibiotics do not penetrate effectively, thus making them more sensitive to current therapeutic doses.

Acknowledgements

The authors thank Prof. Dr. K. Langer, University of Münster, for the HT29-MTX cells and for using Zetasizer**.**

Compliance with Ethical Standards

Ethical Approval: This article does not contain studies with human participants performed by any of the authors.

Funding information

The study had been fully financed from intramural grants of University of Münster (no grant numbers available).

Conflict of Interest

All authors (MG, TS, TM, FG and AH) declare that she/he has no conflict of interest.

Authors‘ contribution

MG performed experiments and made substantial contributions to acquisition, analysis and interpretation of data; TS helped with confocal laser scanning microscopy; TM helped during the liposome preparation; FG was involved in experiments, revised and discussed the MS; AH designed the study and has been involved in drafting and revising the MS.

References

Adamczak MI, Martinsen ØG, Smistad G, Hiorth M (2016) Water sorption properties of HM-pectin and liposomes intended to alleviate dry mouth. Inter J Pharm 506:201–206.

Algood HMS, Cover TL (2006) *Helicobacter pylori* persistence: an overview of interactions between *H. pylori* and host immune defenses. Clin Microbiol Rev 19:597–613.

Angsantikul P, Thamphiwatana S, Zhang Q, Spiekermann K, Zhuang J, Fang RH, Gao W, Obonyo M, Zhang L (2018) Coating nanoparticles with gastric epithelial cell membrane for targeted antibiotic delivery against *Helicobacter pylori* infection. Adv Ther 1:1800016.

Ansari S, Yamaoka Y (2019) *Helicobacter pylori* virulence factors exploiting gastric colonization and its pathogenicity. Toxins 11:677.

Bardonnet P-L, Faivre V, Boullanger P, Piffaretti J-C, Falson F (2008) Pre-formulation of liposomes against *Helicobacter pylori:* characterization and interaction with the bacteria. Eur J Pharm Biopharm 69:908–922

Cao X, Bansil R, Bhaskar KR, Turner BS, LaMont JT, Niu N, Afdhal NH (1999) pH-Dependent conformational change of gastric mucin leads to sol-gel transition. Biophys J 76:1250–1258.

Cho JH, Kwun YS, Jang HS, Kang JM, Won YS, Yoon HR (2000) Long-term use of preservatives on rat nasal respiratory mucosa: effects of benzalkonium chloride and potassium sorbate. Laryngoscope 110:312–317.

Cornick S, Tawiah A, Chadee K (2015) Roles and regulation of the mucus barrier in the gut. Tissue Barriers 3:e982426.

Danaei M, Dehghankhold M, Ataei S, Hasanzadeh Davarani F, Javanmard R, Dokhani A, Khorasani S, Mozafari MR (2018) Impact of particle size and polydispersity index on the clinical applications of lipidic nanocarrier systems. Pharmaceutics 10.

Dragicevic-Curic N, Scheglmann D, Albrecht V, Fahr A (2008) Temoporfin-loaded invasomes: development, characterization and in vitro skin penetration studies. J Contr Rel 127:59–69.

Fredenberg S, Wahlgren M, Reslow M, Axelsson A (2011) The mechanisms of drug release in poly(lactic-co-glycolic acid)-based drug delivery systems-a review. Inter J Pharm 415:34–52.

Gottesmann M, Paraskevopoulou V, Mohammed A, Falcone FH, Hensel A (2020) BabA and LPS inhibitors against *Helicobacter pylori*: pectins and pectin-like rhamnogalacturonans as adhesion blockers. Appl Microbiol Biotechnol 104:351-363.

Goycoolea FM, Morris ER, Gidley MJ (1995) Screening for synergistic interactions in dilute polysaccharide solutions. Carbohydr Polymers 28:351–358.

Guyer W, Bloch K (1983) Phosphatidylcholine and cholesterol interactions in model membranes. Chem Phys Lipids 33:313–322.

Hage N, Howard T, Phillips C, Brassington C, Overman R, Debreczni J, Gellert P, Stolnik S, Winkler GS, Falcone FH (2015) Structural basis of Lewis(b) antigen binding by the *Helicobacter pylori* adhesin BabA. Science Advances 1:e1500315-e1500315.

Hassan EE, Gallo JM (1990) A simple rheological method for the in vitro assessment of mucin-polymer bioadhesive bond strength. Pharm. Res 7:491–495.

Helicobacter and Cancer Collaborative Group (2001) Gastric cancer and *Helicobacter pylori*: a combined analysis of 12 case control studies nested within prospective cohorts. Gut 49:347–353.

Hensel A, Deters AM, Müller G, Stark T, Wittschier N, Hofmann T (2007) Occurrence of *N*-phenylpropenoyl-L-amino acid amides in different herbal drugs and their

influence on human keratinocytes, on human liver cells and on adhesion of *Helicobacter pylori* to the human stomach. Planta Med 73:142–150.
Herrmann A, König S, Lechtenberg M, Sehlbach M, Vakhrushev SY, Peter-Katalinic J, Hensel A (2012) Proteoglycans from *Boswellia serrata* Roxb. and *B. carteri* Birdw. and identification of a proteolytic plant basic secretory protein. Glycobiology 22:1424–1439.
International Agency for Research on Cancer IARC Working Group on the Evaluation of Carcinogenic Risks to Humans (1994) Schistosomes, liver flukes and *Helicobacter pylori*. Lyon, France, International Agency for Research on Cancer. IARC Monographs on the Evaluation of Carcinogenic Risks to Humans, 61.
Lesuffleur T, Porchet N, Aubert JP, Swallow D, Gum JR, Kim YS, Real FX, Zweibaum A (1993) Differential expression of the human mucin genes MUC1 to MUC5 in relation to growth and differentiation of different mucus-secreting HT-29 cell subpopulations. J Cell Sci 106 (Pt 3):771–783.
Lin Y-H, Tsai S-C, Lai C-H, Lee C-H, He ZS, Tseng G-C (2013) Genipin-cross-linked fucose-chitosan/heparin nanoparticles for the eradication of *Helicobacter pylori*. Biomaterials 34:4466–4479.
Malfertheiner P, Megraud F, O'Morain CA, Gisbert JP, Kuipers EJ, Axon AT, Bazzoli F, Gasbarrini A, Atherton J, Graham DY, Hunt R, Moayyedi P, Rokkas T, Rugge M, Selgrad M, Suerbaum S, Sugano K, El-Omar EM (2017) Management of *Helicobacter pylori* infection – the Maastricht V/Florence Consensus Report. Gut. 66: 6–30.
Menchicchi B, Fuenzalida JP, Bobbili KB, Hensel A, Swamy MJ, Goycoolea FM (2014) Structure of chitosan determines its interactions with mucin. Biomacromolecules 15:3550–3558.
Menchicchi B, Fuenzalida JP, Hensel A, Swamy MJ, David L, Rochas C, Goycoolea FM (2015a) Biophysical analysis of the molecular interactions between polysaccharides and mucin. Biomacromolecules 16:924–935.
Menchicchi B, Hensel A, Goycoolea FM (2015b) Polysaccharides as bacterial antiadhesive agents and „smart" constituents for improved drug delivery systems against *Helicobacter pylori* infection. Cur Pharm Des 21:4888–4906.
Menchicchi B, Savvaidou E, Thöle C, Hensel A, Goycoolea FM (2019) Low-molecular-weight dextran sulfate nanocapsules inhibit the adhesion of *Helicobacter pylori* to gastric cells. ACS Appl. Bio Mater. 2:4777–4789.
Messing J, Niehues M, Shevtsova A, Borén T, Hensel A (2014) Antiadhesive properties of arabinogalactan protein from *Ribes nigrum* seeds against bacterial adhesion of *Helicobacter pylori*. Molecules 19:3696–3717.
Mosmann T (1983) Rapid colorimetric assay for cellular growth and survival: Application to proliferation and cytotoxicity assays. J Immunol Meth 65:55–63.
Mysore JV, Wigginton T, Simon PM, Zopf D, Heman-Ackah LM, Dubois A (1999) Treatment of *Helicobacter pylori* infection in rhesus monkeys using a novel antiadhesion compound. Gastroenterology 117:1316–1325.
Narożańska E, Białecka M, Adamiak-Giera U, Gawrońska-Szklarz B, Sołtan W, Schinwelski M, Robowski P, Madaliński MH, Sławek J (2014) Pharmacokinetics of levodopa in patients with Parkinson disease and motor fluctuations depending on the presence of *Helicobacter pylori* infection. Clin Neuropharmacol 37:96–99.
Niehues M, Euler M, Georgi G, Mank M, Stahl B, Hensel A (2010) Peptides from *Pisum sativum* L. enzymatic protein digest with anti-adhesive activity against *Helicobacter pylor*i: structure-activity and inhibitory activity against BabA, SabA, HpaA and a fibronectin-binding adhesin. Mol Nutr Food Res 54:1851–1861.
Niehues M, Hensel A (2009) In-vitro interaction of L-dopa with bacterial adhesins of *Helicobacter pylori:* an explanation for clinicial differences in bioavailability? J Pharm Pharmacol 61:1303–1307.

Nogueira F, Gonçalves IC, Martins MCL (2013) Effect of gastric environment on *Helicobacter pylori* adhesion to a mucoadhesive polymer. Acta Biomat 9:5208–5215.

Parente F, Cucino C, Anderloni A, Grandinetti G, Porro GB (2003) Treatment of *Helicobacter pylori* infection using a novel antiadhesion compound (3'sialyllactose sodium salt). A double blind, placebo-controlled clinical study. Helicobacter 8:252–256.

Qin X, Engwer C, Desai S, Vila-Sanjurjo C, Goycoolea FM (2017) An investigation of the interactions between an *E. coli* bacterial quorum sensing biosensor and chitosan-based nanocapsules. Coll Surf B, Biointerfaces 149:358–368.

Ramteke S, Ganesh N, Bhattacharya S, Jain NK (2008) Triple therapy-based targeted nanoparticles for the treatment of *Helicobacter pylori*. J Drug Target 16:694–705.

Rowland RN, Woodley JF (1980) The stability of liposomes in vitro to pH, bile salts and pancreatic lipase. Biochim Biophysica Acta Lipids and Lipid Metabolism 620:400–409.

Sehlbach M, König S, Mormann M, Sendker J, Hensel A (2013) Arabinogalactan protein cluster from *Jatropha curcas* seed embryo contains fasciclin, xylogen and LysM proteins. Carbohydr Polymers 98:522–531.

Shmuely H, Burger O, Neeman I, Yahav J, Samra Z, Niv Y, Sharon N, Weiss E, Athamna A, Tabak M, Ofek I (2004) Susceptibility of *Helicobacter pylori* isolates to the antiadhesion activity of a high-molecular-weight constituent of cranberry. Diagn Microbiol Infectious Dis 50:231–235.

Sitarz R, Skierucha M, Mielko J, Offerhaus GJA, Maciejewski R, Polkowski WP (2018) Gastric cancer: epidemiology, prevention, classification, and treatment. Cancer Manag Res 10:239–248.

Trampenau C, Müller K-D (2003) Affinity of *Helicobacter pylori* to cholesterol and other steroids. Micr Infect 5:13–17.

Waigh TA, Papagiannopoulos A, Voice A, Bansil R, Unwin AP, Dewhurst CD, Turner B, Afdhal N (2002) Entanglement coupling in porcine stomach mucin. Langmuir 18:7188–7195.

Weissman G, SESSA G, Weismann S (1965) Effect of steroids and 'Triton X-100' on glucose-filled phospholipid/cholesterol structures. Nature 208:649–651.

Wittschier N, Faller G, Hensel A (2009) Aqueous extracts and polysaccharides from liquorice roots (*Glycyrrhiza glabra* L.) inhibit adhesion of *Helicobacter pylori* to human gastric mucosa. J Ethnopharmacol 125:218–223.

Wittschier N, Lengsfeld C, Vorthems S, Stratmann U, Ernst JF, Verspohl EJ, Hensel A (2007) Large molecules as anti-adhesive compounds against pathogens. J Pharm Pharmacol 59:777–786.

WHO (2017) https://www.who.int/en/news-room/detail/27-02-2017-who-publishes-list-of-bacteria-for-which-new-antibiotics-are-urgently-needed. Last access 25. March 2010.

Zamani M, Ebrahimtabar F, Zamani V, Miller WH, Alizadeh-Navaci R, Shokri-Shirvani J, Derakhshan MH (2018) Systematic review with meta-analysis: the worldwide prevalence of *Helicobacter pylori* infection. Aliment Pharmacol Ther 47:868-152.

Figures and Table Captions

Captions to Figures

Fig 1 Stability of (**A**) uncoated, amoxicillin loaded liposomes (UCL_A) and (**B**) coated, amoxicillin loaded liposomes (CL_A) in simulated gastric fluid (SGF; pH = 1.2) over 24 h at 37 °C. Data represent the mean ± SD from n = 2 independent experiments with 3 technical replicates. ***: $p < 0.001$, **: $p < 0.01$, *: $p < 0.05$

Fig 2 Relative cell viability of AGS cells after incubation with different concentrations of liposomes for 2 h, as determined by MTT assay. UC: untreated control: AGS medium without supplementation, PC: positive control: AGS medium supplemented with 10 % FCS, NC: negative control (AGS medium supplemented with 20 % DMSO); values are mean ± SD, n = 3 independent experiments with 6 technical replicates each. ***: $p < 0.001$, **: $p < 0.01$

Fig 3 Influence of different liposome formulations on the relative cell viability of HT29-MTX cells during their growing phase (**A**) and in the respective mucus-secreting phase (**B**), as determined by MTT assay. UCL, CL, UCL_A, CL_A were tested at different concentrations and incubated with cells for 2 h. UC: untreated control: $PBS^{+/+}$, PC: positive control: $PBS^{+/+}$ supplemented with 10 % FCS, NC: negative control: $PBS^{+/+}$ supplemented with 20 % DMSO; values are mean ± SD, n = 3 independent experiments with 6 technical replicates each. ***: $p < 0.001$, *: $p < 0.05$

Fig 4 Influence of porcine mucin on size and PDI (**A**, **C**) and zeta potential (**B**, **D**) of uncoated, amoxicillin loaded liposomes (UCL_A) and coated, amoxicillin loaded liposomes (CL_A). Liposomes were mixed with mucin (0.4 mg/mL) in a ratio of 1:1 at RT (**A**, **B**) or liposomes were incubated with mucin (0.2 mg/mL) for 2 h at 37 °C under shaking (**C**, **D**). Results are obtained from a single experiment with three technical replicates

Fig 5 Relative mucus interaction (% related to untreated control, UC = 100 %, corresponds to the total fluorescence of DiD-labelled liposomes UCL_DiD and CL_DiD) of uncoated DiD-labelled liposomes (UCL_DiD, left) and coated, DiD-labelled liposomes (CL_DiD, right) with mucus, secreted by HT29-MTX cells. Cells were incubated at 37 °C for 2 h together with liposomes in a concentration range from 0.01 to 1 mg/mL

Fig 6 Representative fluorescence microscopy images of FITC-labelled *H. pylori* (**A**), UCL_DiD liposomes (**B**), UCL_DiD mixed with *H. pylori* (**C**), and CL_DiD mixed with *H. pylori* (**D**).

Fig 7 Orthogonal projection of CLSM images of AGS cells incubated with *H. pylori* and liposomes (UCL: uncoated liposomes; CL: coated liposomes). Cell nuclei are stained with DAPI (blue), bacteria with FITC (green), and liposomes with DiD (red); scale bar: 5 µm

Fig 8 3D image reconstructions from CLSM image series of AGS cells and *H. pylori*, incubated with uncoated UCL_DiD (**A**) and coated CL_DiD (**B**) liposomes. DNA is coloured blue (DAPI), bacteria green (FITC), and liposomes red (DiD)

Fig 9 Representative CLSM images of potential interactions between *H. pylori* and uncoated UC_DiD (**A**) and coated CL_DiD (**B**) liposomes. DNA of bacteria was stained with DAPI (light blue) and liposomes with DiD (red). Scale bar: 5 µm

Table 1.

Table 1 Physicochemical characterization of pectin-coated (CL) and uncoated (UCL) liposomes, and the corresponding DiD-labelled formulations

	Zeta average size (d, nm)	Polydispersity index	Zeta potential (mV)
UCL	178 ± 44	0.204 ± 0.091	+ 44.1 ± 4.3
CL	529 ± 73	0.300 ± 0.100	− 27.9 ± 3.8
UCL_A	149 ± 8	0.164 ± 0.047	+ 44.2 ± 2.9
CL_A	517 ± 26	0.291 ± 0.023	− 26.9 ± 5.1
UCL_DiD	140 ± 11	0.147 ± 0.007	+ 43.4 ± 5.0
CL_DiD	432 ± 7	0.292 ± 0.011	− 24.1 ± 0.9

Figure 1.

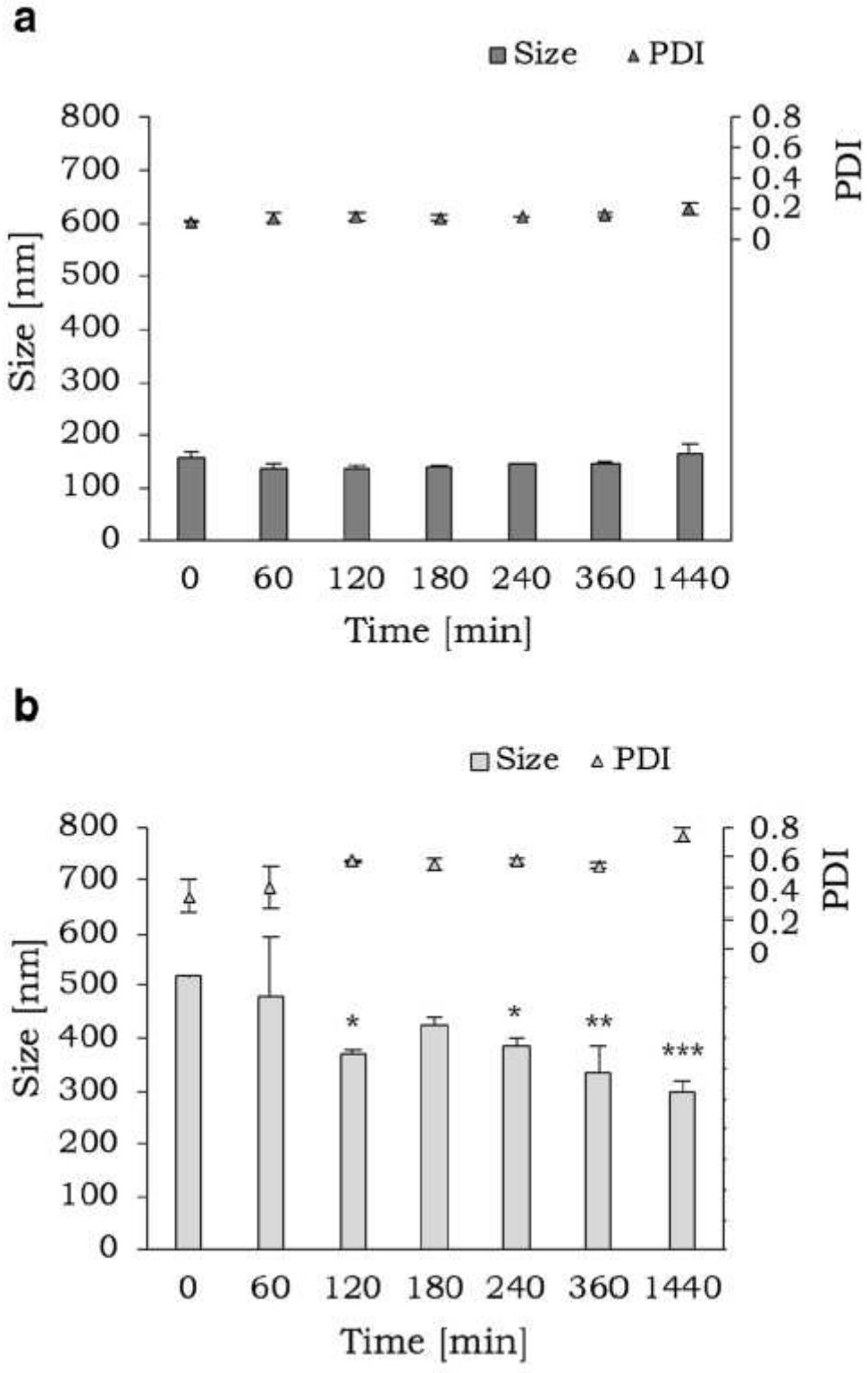
a
Size
PDI
800
700
600
500
400
300
200
100
0
Size [nm]
0.8
0.6
0.4
0.2
0
PDI
0
60
120
180
240
360
1440
Time [min]
b
Size
PDI
800
700
600
500
400
300
200
100
0
Size [nm]
0.8
0.6
0.4
0.2
0
PDI
*
*
**
***
0
60
120
180
240
360
1440
Time [min]

Figure 2.

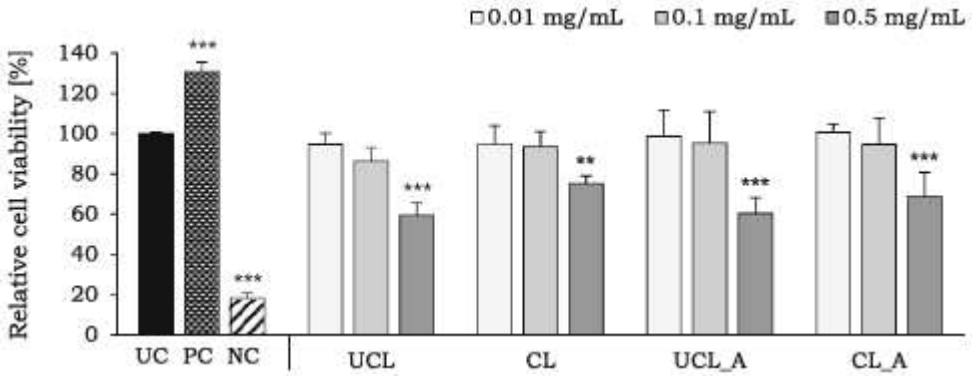
0.01 mg/mL
0.1 mg/mL
0.5 mg/mL
Relative cell viability [%]
140
120
100
80
60
40
20
0
***
***
***
**
***
***
UC
PC
NC
UCL
CL
UCL_A
CL_A

Figure 3.

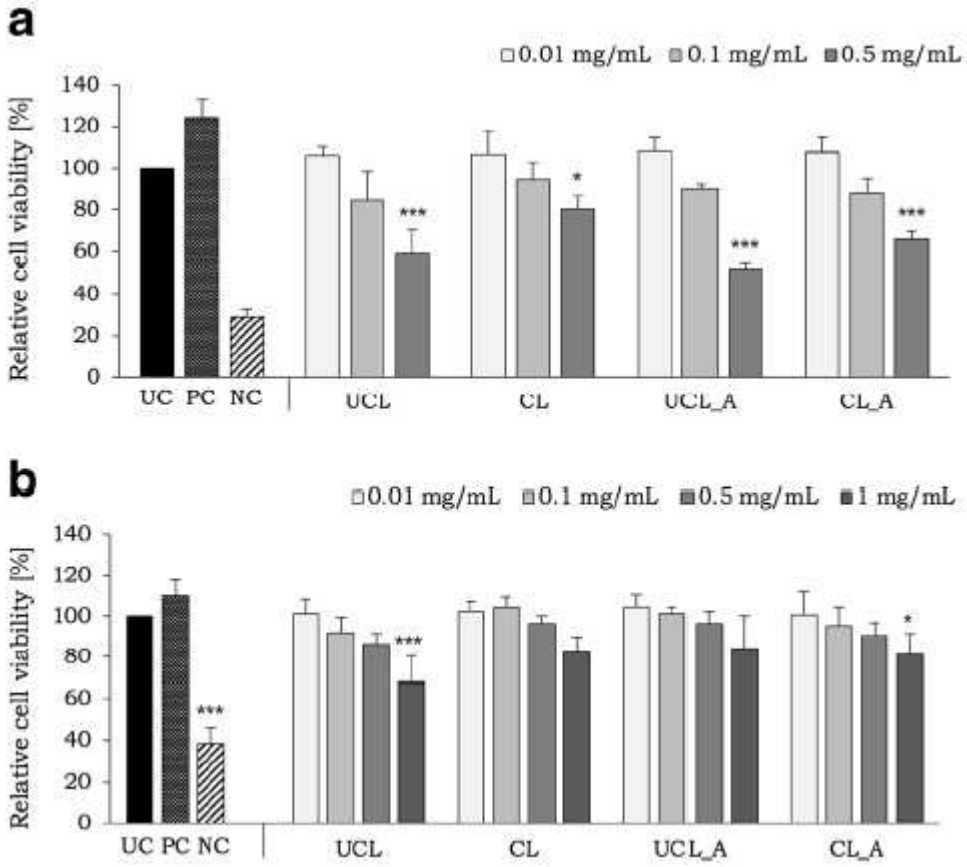
a
0.01 mg/mL
0.1 mg/mL
0.5 mg/mL
Relative cell viability [%]
140
120
100
80
60
40
20
0
UC
PC
NC
UCL
CL
UCL_A
CL_A
b
0.01 mg/mL
0.1 mg/mL
0.5 mg/mL
1 mg/mL
Relative cell viability [%]
UC PC NC
UCL
CL
UCL_A
CL_A

Figure 4.

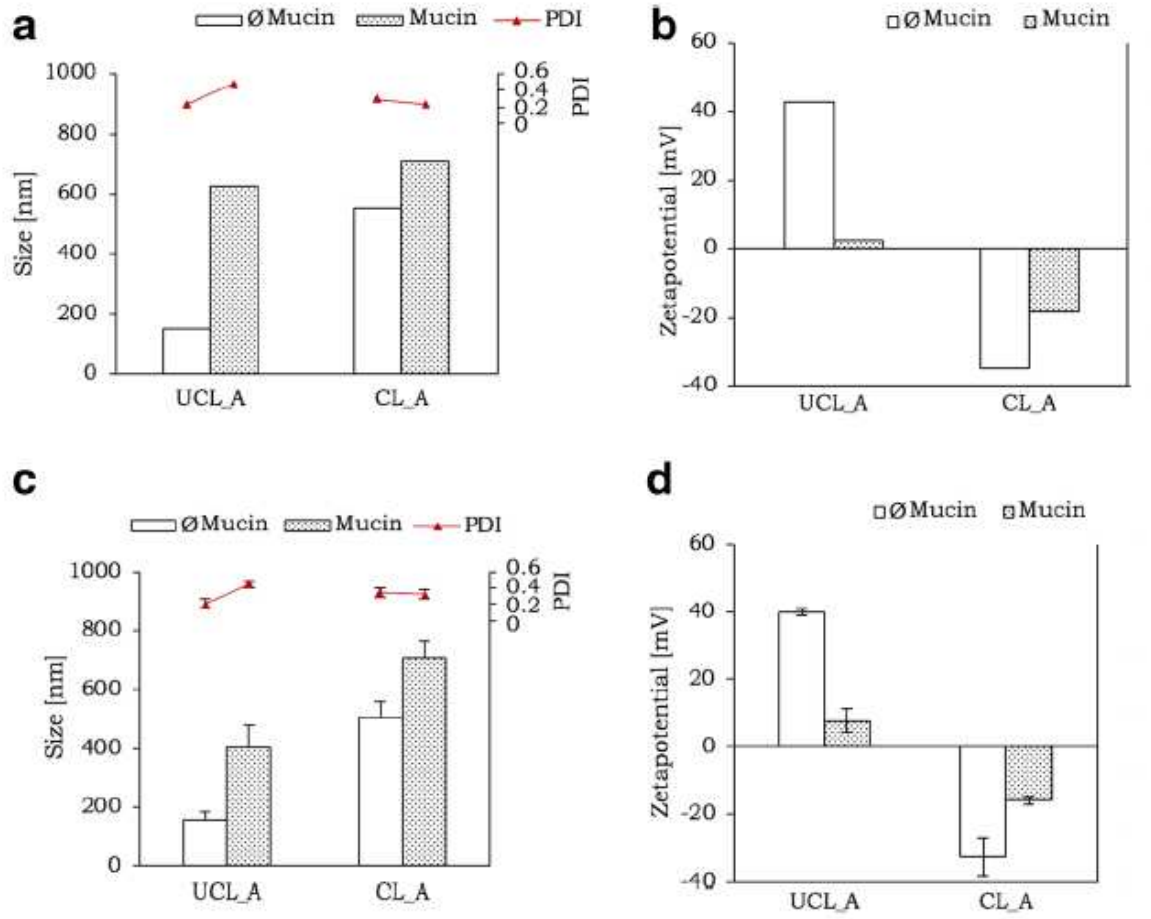
a
Ø Mucin
Mucin
PDI
Size [nm]
1000
800
600
400
200
0
0.6
0.4
0.2
0
PDI
UCL_A
CL_A
b
Ø Mucin
Mucin
Zetapotential [mV]
60
40
20
0
-20
-40
UCL_A
CL_A
c
Ø Mucin
Mucin
PDI
Size [nm]
1000
800
600
400
200
0
0.6
0.4
0.2
0
PDI
UCL_A
CL_A
d
Ø Mucin
Mucin
Zetapotential [mV]
60
40
20
0
-20
-40
UCL_A
CL_A

Figure 5.

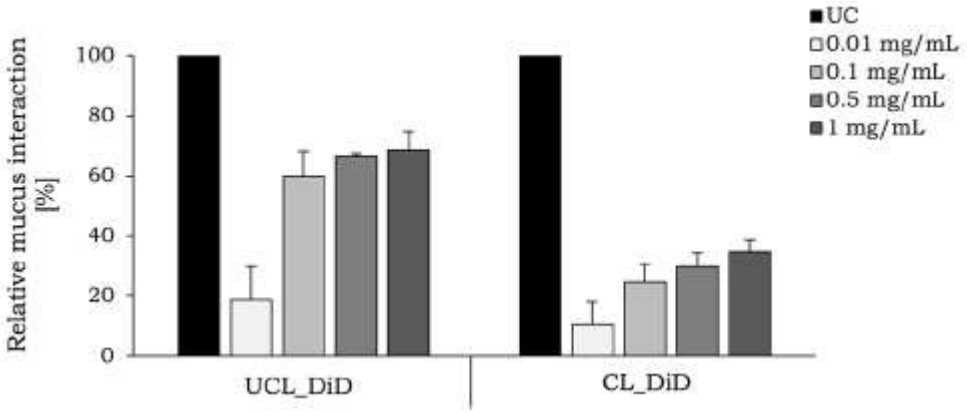
Relative mucus interaction [%]
100
80
60
40
20
0
UCL_DiD
CL_DiD
UC
0.01 mg/mL
0.1 mg/mL
0.5 mg/mL
1 mg/mL

Figure 6.

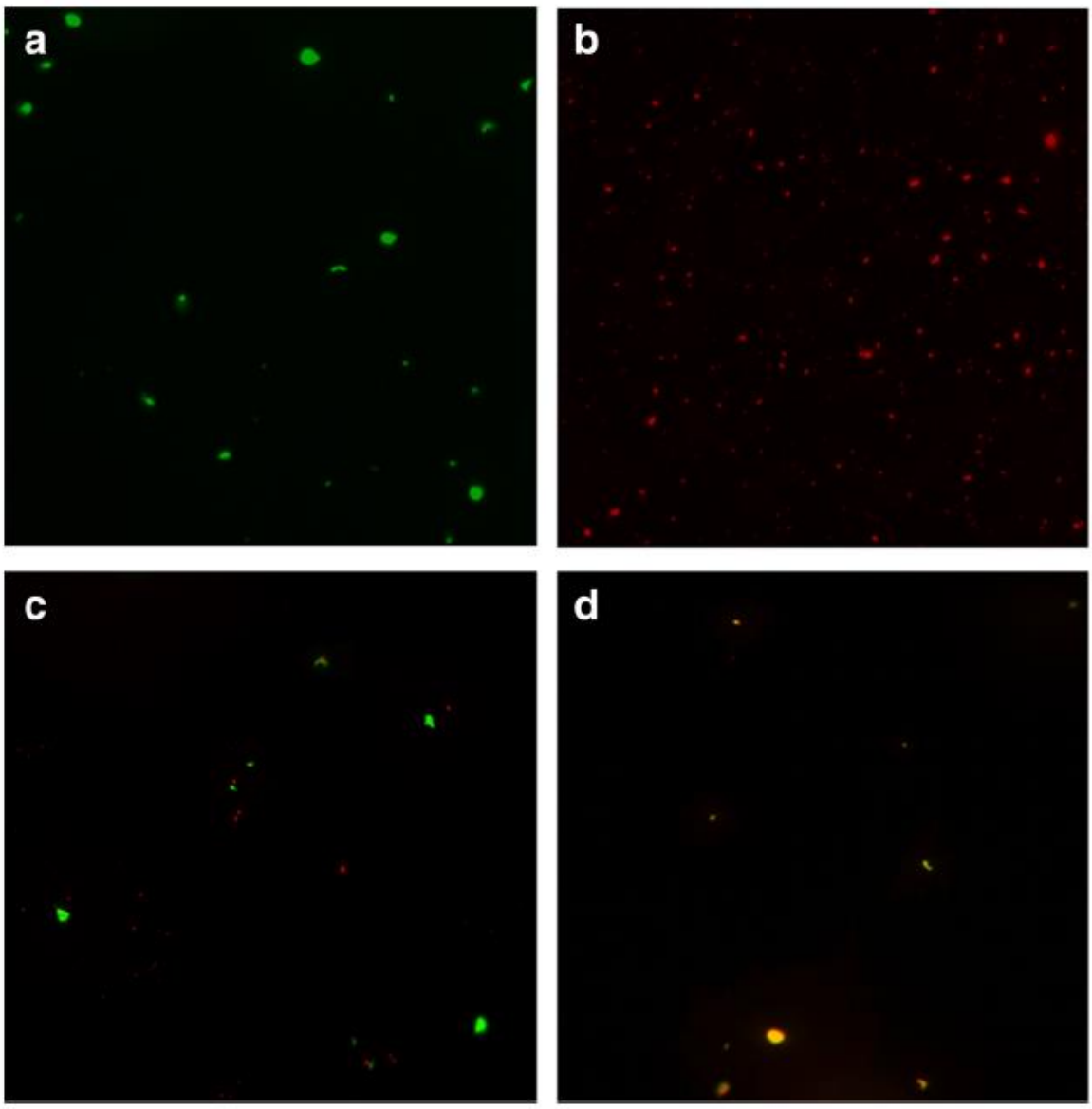

Figure 7.

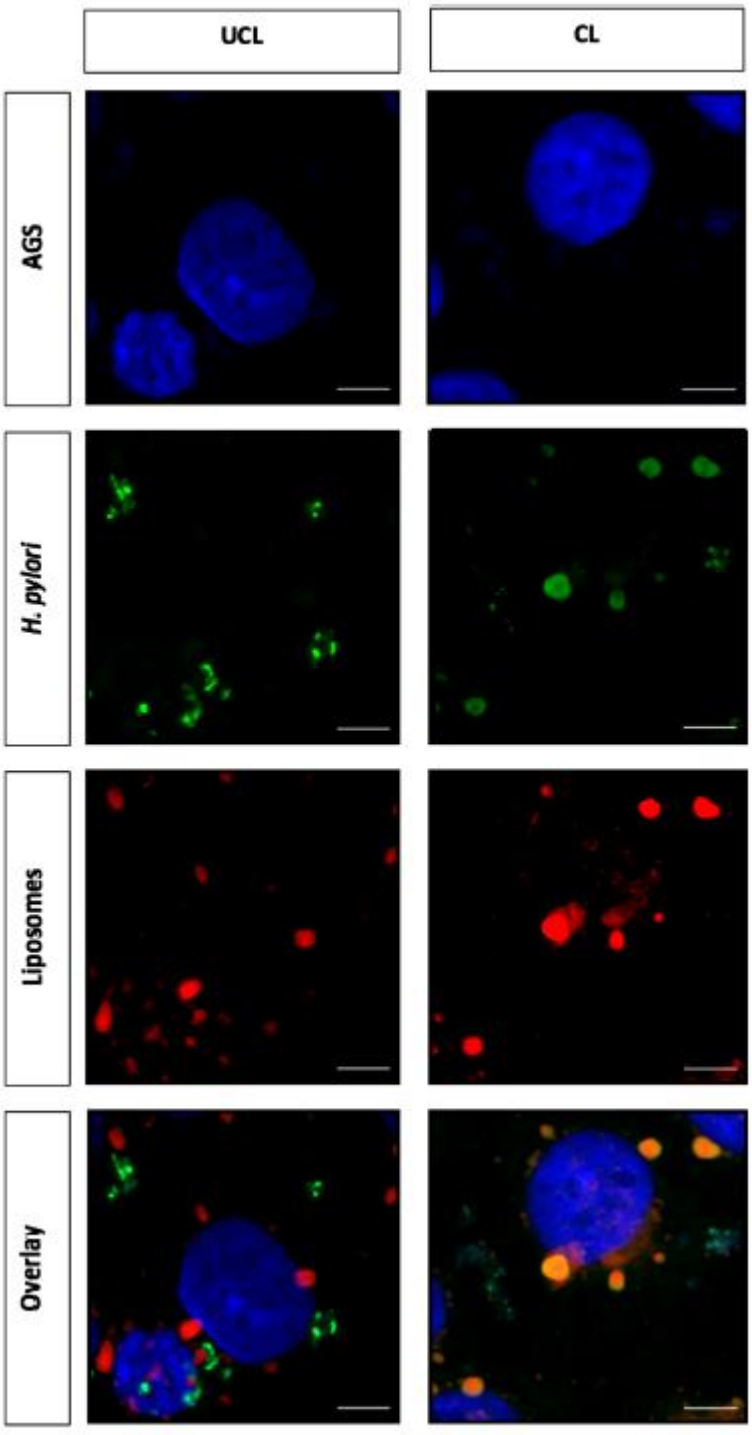

Figure 8.

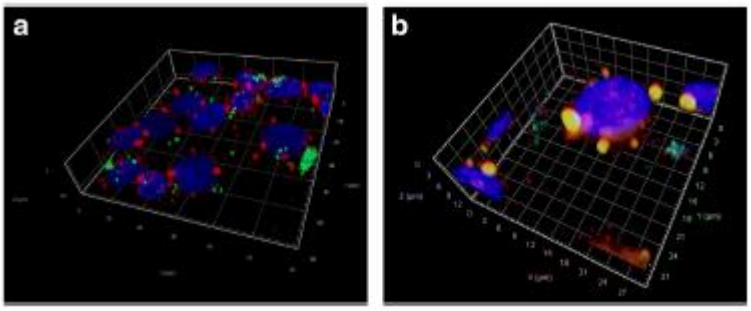

Figure 9.